Stanford Exploration Project, Report 77, November 17, 1997, pages 289–303

Stanford Exploration Project, Report 77, November 17, 1997, pages 289–303

Applications of two-D deconvolution

Ray Abma and Jon Claerbout[1]

keywords: *deconvolution, two-dimensional*

ABSTRACT

We've found that Burg's two-dimensional filter offers too much freedom in producing lateral predictions, since the predictions within a trace appear to overwhelm the lateral predictions. Instead, we fix the filter coefficients along the output column so the form of the two-dimensional filter becomes equivalent to that of the FX-decon operator. The ability to control the length of this filter in time allows two-dimensional deconvolution to produce a result superior to the FX-decon result. A symmetry for operators calculated forward and backward in space has been found, but it only applies for filters with no free elements in the output column of that filter. The filter shapes of other two-dimensional deconvolution filters are compared and filter shapes that might allow new applications are outlined.

INTRODUCTION

An early version of two-dimensional deconvolution was the FX-decon process developed by Canales(1984). This two-dimensional deconvolution was done by using a one-dimensional filter within each frequency in the frequency-space domain. Burg (Claerbout, 1992b) established the form of a two-dimensional prediction-error filter that would whiten the two-dimensional spectrum of its output. Claerbout(1992) specialized Burg's filter to remove plane waves from a seismic section with a process referred to as LOMOPLAN.

Here, we specialize Burg's filter to do a lateral prediction that will be equivalent to the FX-decon process by using a modification of Claerbout's LOMOPLAN program. We show that FX-decon is almost equivalent to lateral prediction with two-dimensional deconvolution, and that the added ability of two-dimensional deconvolution to control the length of this filter in time gives us a result that should be superior to the FX-decon result. A symmetry for the two-dimensional deconvolution operators calculated forward and backward in space that will save filter calculation time is also found. We also review some of the effects of different filter sizes and shapes and speculate about the uses of other filter configurations.

[1]**email:** not available

Burg's two-dimensional filter offered too much freedom to produce good lateral predictions, because the predictions within a trace overwhelmed the lateral predictions. By fixing the filter coefficients along the output column, we avoided the strong predictions within a trace and also found the form of the two-dimensional filter then became equivalent to that of the FX-decon operator. We show a method of producing better results than FX-decon by using lateral prediction with two-dimensional deconvolution and derive a two-dimensional filter from the collection of the FX-decon operators. Other two-dimensional deconvolution applications are also reviewed. These multi-dimensional filters appear to have a flexibility that other techniques do not. We are now beginning to understand what the possibilities and limitations are. The capability of choosing a filter shape to control the action of the filter may allow many new applications with seismic data.

A LATERAL-PREDICTION FILTER APPLICATION

Filter shape considerations

Rather than using two-dimensional deconvolution for a prediction-error filter as in the LOMOPLAN case above, Ray Abma (1993) used two-dimensional deconvolution to predict and to keep events that were laterally continuous. The process is used to eliminate noise from a seismic section in a manner similar to FX-decon(Canales, 1984),(Gulunay, 1986). Two-dimensional deconvolution is more constrained than FX-decon since two-dimensional deconvolution is done in the time domain with a limited number of filter coefficients, while FX-decon is done separately within each frequency, making the number of filter coefficients fairly large.

The first filter we used for lateral prediction was simply Burg's two-dimensional filter using several columns to predict multiple linear events. This filter appeared as:

$$\begin{array}{ccccc} a_{11} & a_{12} & a_{13} & a_{14} & a_{15} \\ a_{21} & a_{22} & a_{23} & a_{24} & a_{25} \\ 1 & a_{32} & a_{33} & a_{34} & a_{35} \\ \cdot & a_{42} & a_{43} & a_{44} & a_{45} \\ \cdot & a_{52} & a_{53} & a_{54} & a_{55} \end{array} . \tag{1}$$

Here and for the other filters displayed, the vertical axis is the time axis, the horizontal axis is the space axis. For clarity, zeros are indicated by "·"s.

The filter coefficients are calculated using a conjugate-gradient technique described in Claerbout (1992) . Generally, three coefficients in the time direction were found to be sufficient, but more may be needed if steep dips are found.

The results of the lateral prediction process using this filter was usually comparable to the results of FX-decon, but we found one case where FX-decon was producing a much better result than the two-dimensional deconvolution process. This case involved a global image provided to us by Shearer(1991). To improve our result, Jon

Claerbout suggested that the modified filter shown in Filter (2) would produce better results than Filter (1).

$$\begin{array}{ccccc} \cdot & a_{12} & a_{13} & a_{14} & a_{15} \\ \cdot & a_{22} & a_{23} & a_{24} & a_{25} \\ 1 & a_{32} & a_{33} & a_{34} & a_{35} \\ \cdot & a_{42} & a_{43} & a_{44} & a_{45} \\ \cdot & a_{52} & a_{53} & a_{54} & a_{55} \end{array} . \tag{2}$$

The difference between Filters (1) and (2) is that the first column of Filter (2) does not contain any free coefficients. This would prevent any prediction done along the time axis in the traces. The predictions within a trace are probably so great that the lateral predictions become unimportant. For example, a noisy trace would be well predicted if the prediction along the time axis was good, even if no prediction could be done laterally. The results of applying these two filters to the problem case are compared later and may be seen in Figures 3 and 4. The calculated filters are show below in Filters (4) to (7) and Figures 1 and 2 as a seismic plot.

The equivalence of the constrained two-D filter and FX-decon

The similarity in the results of applying Filter (2) and applying FX-decon may be explained by the Fourier transform of the FX-decon operators. FX-decon calculates a separate filter within each frequency of the form

$$1 \quad a_2 \quad a_3 \quad a_4 \quad a_5 \ . \tag{3}$$

If these filters were transformed from the frequency-space domain into the time-space domain, they would appear as a single two-dimensional filter. The collection of these

filters in the frequency-space domain
$$\begin{array}{ccccc} 1 & a & a & a & a \\ 1 & a & a & a & a \\ 1 & a & a & a & a \\ 1 & a & a & a & a \\ 1 & a & a & a & a \\ 1 & a & a & a & a \\ 1 & a & a & a & a \\ 1 & a & a & a & a \\ 1 & a & a & a & a \\ 1 & a & a & a & a \\ 1 & a & a & a & a \\ 1 & a & a & a & a \\ 1 & a & a & a & a \\ 1 & a & a & a & a \\ 1 & a & a & a & a \\ 1 & a & a & a & a \\ 1 & a & a & a & a \end{array}$$
transforms to
$$\begin{array}{ccccc} \cdot & a & a & a & a \\ \cdot & a & a & a & a \\ \cdot & a & a & a & a \\ \cdot & a & a & a & a \\ \cdot & a & a & a & a \\ \cdot & a & a & a & a \\ \cdot & a & a & a & a \\ \cdot & a & a & a & a \\ 1 & a & a & a & a \\ \cdot & a & a & a & a \\ \cdot & a & a & a & a \\ \cdot & a & a & a & a \\ \cdot & a & a & a & a \\ \cdot & a & a & a & a \\ \cdot & a & a & a & a \\ \cdot & a & a & a & a \\ \cdot & a & a & a & a \end{array}$$
in the time-space domain, where the number of rows is the number of time samples

in the window being considered. (The subscripts are omitted for simplicity.) The previous time-space filter is the same as Filter (2) except for the number of rows. It might be expected that the prediction would be limited to elements close to the center of the filter, since events far from the output point are unlikely to affect data at the output position, but correlations for events widely separated in time will create problems with incorrect lineups in the output of FX-decon.

To keep the calculation and application of the filters symmetrical, the two-dimensional deconvolution examples shown in this paper have two filters calculated and applied within each window: one forward in space and one reversed. The filters are not extended beyond times where a full filter response is available, so the two-dimensional deconvolution results shown here have the original data at the top and bottom of the section.

For the type operator shown in Filter (1), the filter calculated for the forward prediction was

$$\begin{array}{ccccc} 0.4564 & -0.2629 & -0.01173 & 0.1009 & 0.03535 \\ 1 & -0.02676 & 0.1169 & 0.121 & 0.04788 \\ 0 & 0.1422 & 0.06668 & 0.06372 & 0.04849 \end{array} \tag{4}$$

and for the reverse prediction, the filter calculated was

$$\begin{array}{ccccc} 0.4958 & 0.004744 & 0.03781 & 0.07075 & 0.04285 \\ 1 & -0.2847 & -0.03107 & 0.0834 & 0.05511 \\ 0 & -0.2811 & -0.1534 & 0.02327 & 0.05016 \end{array} . \tag{5}$$

For simplicity, I will refer to this type of filter, with free coefficients in the output column, as the a_{11}-free filter.

For a filter of the type shown in Filter (2), the filter calculated appears as

$$\begin{array}{ccccc} 0 & -0.2853 & -0.1097 & 0.05663 & 0.02574 \\ 1 & -0.1428 & 0.04498 & 0.08424 & 0.02693 \\ 0 & 0.1136 & 0.02811 & 0.0521 & 0.03426 \end{array} \tag{6}$$

for the forward prediction, and

$$\begin{array}{ccccc} 0 & 0.1136 & 0.02811 & 0.0521 & 0.03426 \\ 1 & -0.1428 & 0.04498 & 0.08424 & 0.02693 \\ 0 & -0.2853 & -0.1097 & 0.05663 & 0.02574 \end{array} \tag{7}$$

for the reverse prediction. I will refer to this filter as the a_{11}-constrained filter.

Notice that the forward and reverse predictions are symmetric in the case of the a_{11}-constrained type filter but not for the a_{11}-free filter. Plots of the filters are shown in Figures 1 and 2.

Now compare the results of the previous two filter shapes on the data that show the greatest difference when used with the a_{11}-free filter and the a_{11}-constrained filter.

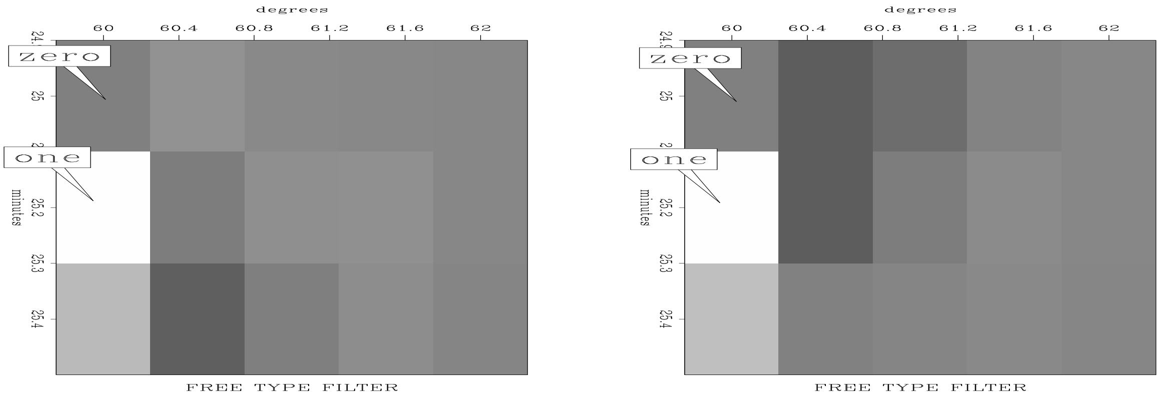

Figure 1: A calculated a_{11}-free filter. The left side is the forward filter, and the right side is the reverse filter. Push the button for a movie of the filters for each iteration of the filter design process. ray2-lomofilt [ER]

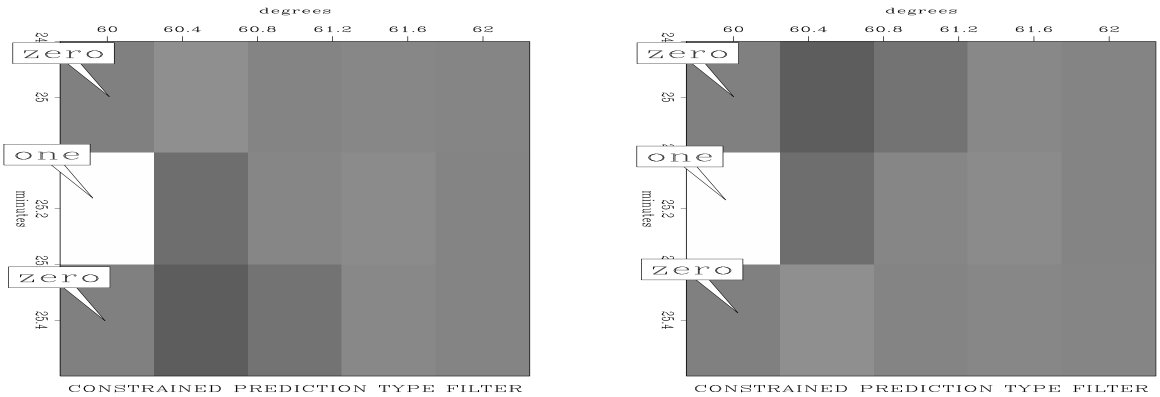

Figure 2: A calculated a_{11}-constrained filter. The left side is the forward filter, and the right side is the reverse filter. Push the button for a movie of the filters for each iteration of the filter design process. ray2-latrfilt [ER]

The result using the a_{11}-constrained filter is shown in Figure 3. The a_{11}-free filter result is shown in Figure 4. Figure 4 shows that the a_{11}-free filter has passed much more noise than the a_{11}-constrained filter. Finally, we show Shearer's full dataset in Figure 5. The two-dimensional deconvolution filter using the a_{11}-constrained filter has eliminated most of the random noise in the input section. Examples of comparisons between FX-decon and lateral prediction with two-dimensional deconvolution are shown in another paper in this volume (Abma, 1993).

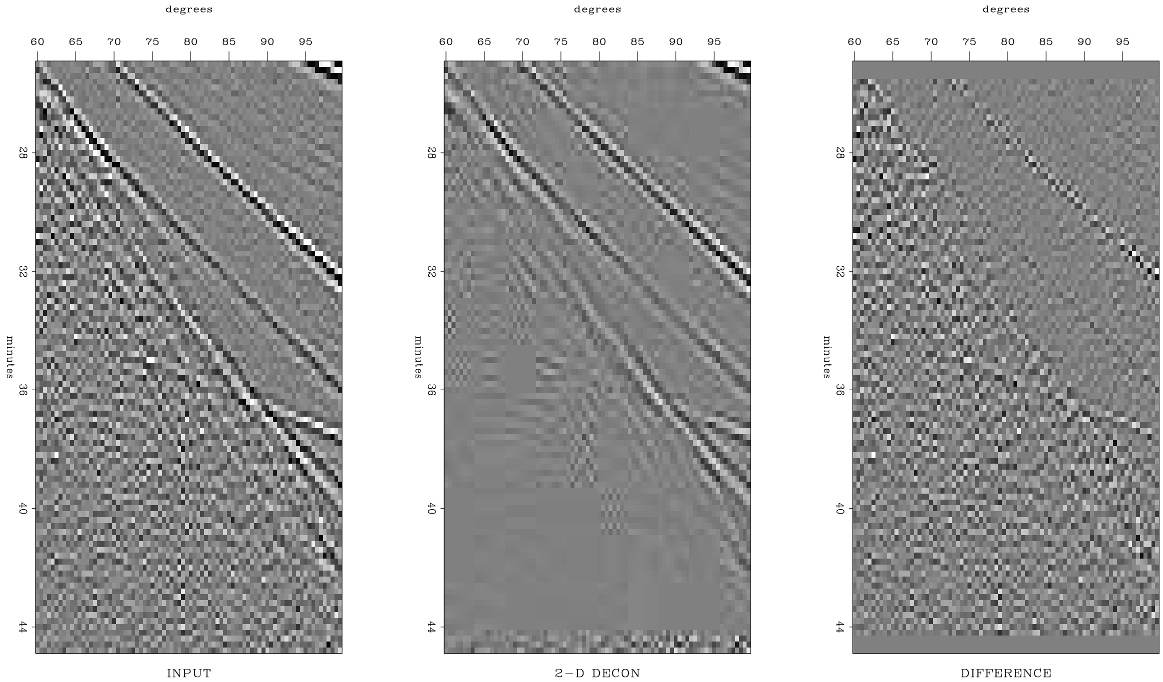

Figure 3: Two-D deconvolution filtering of the horizontal component of Shearer's global image dataset with the a_{11}-constrained filter. ray2-trans [ER]

OTHER APPLICATIONS OF TWO-D DECONVOLUTION

2-D local-mono-plane wave annihilation

An early application of two-dimensional deconvolution was Claerbout's modification of Burg's two-dimensional filter to remove single plane waves from a dataset (Claerbout, 1992b). This modification constrained the filter to two columns so that only one linear event would be removed. After the plane waves were removed from a seismic section, events of interest such as faults, pinchouts, and migration artifacts would remain. This process was called LOMOPLAN for local mono plane annihilator.

The filter used in LOMOPLAN is shown below as Filter (8). The filter has only

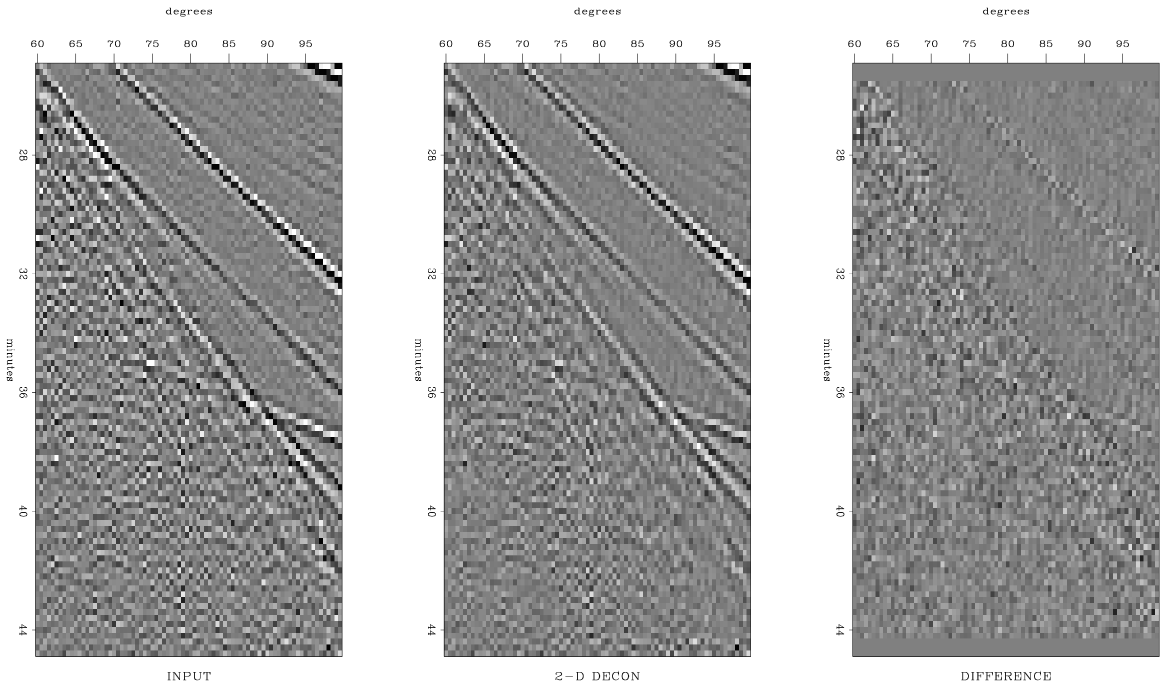

Figure 4: Two-D deconvolution filtering of the horizontal component of Shearer's global image dataset using the a_{11}-free filter. ray2-transy [ER]

two columns that limit it to predicting and removing only one event in a window.

$$\begin{array}{cc} a_{11} & a_{12} \\ a_{21} & a_{22} \\ 1 & a_{32} \\ \cdot & a_{42} \\ \cdot & a_{52} \end{array} \tag{8}$$

2-dimensional LOMOPLAN is used as a prediction-error filter, where the events of interest are those that are unpredictable. While the predicted events are just the difference between the input and the prediction-error output, the LOMOPLAN process stresses what cannot be predicted.

Steep-dip deconvolution

The most recent application is Jon Claerbout's (1993) steep-dip deconvolution work. This approach involves predicting and removing undesired events, as opposed to predicting the desired events and disregarding everything else. These filters have a shape

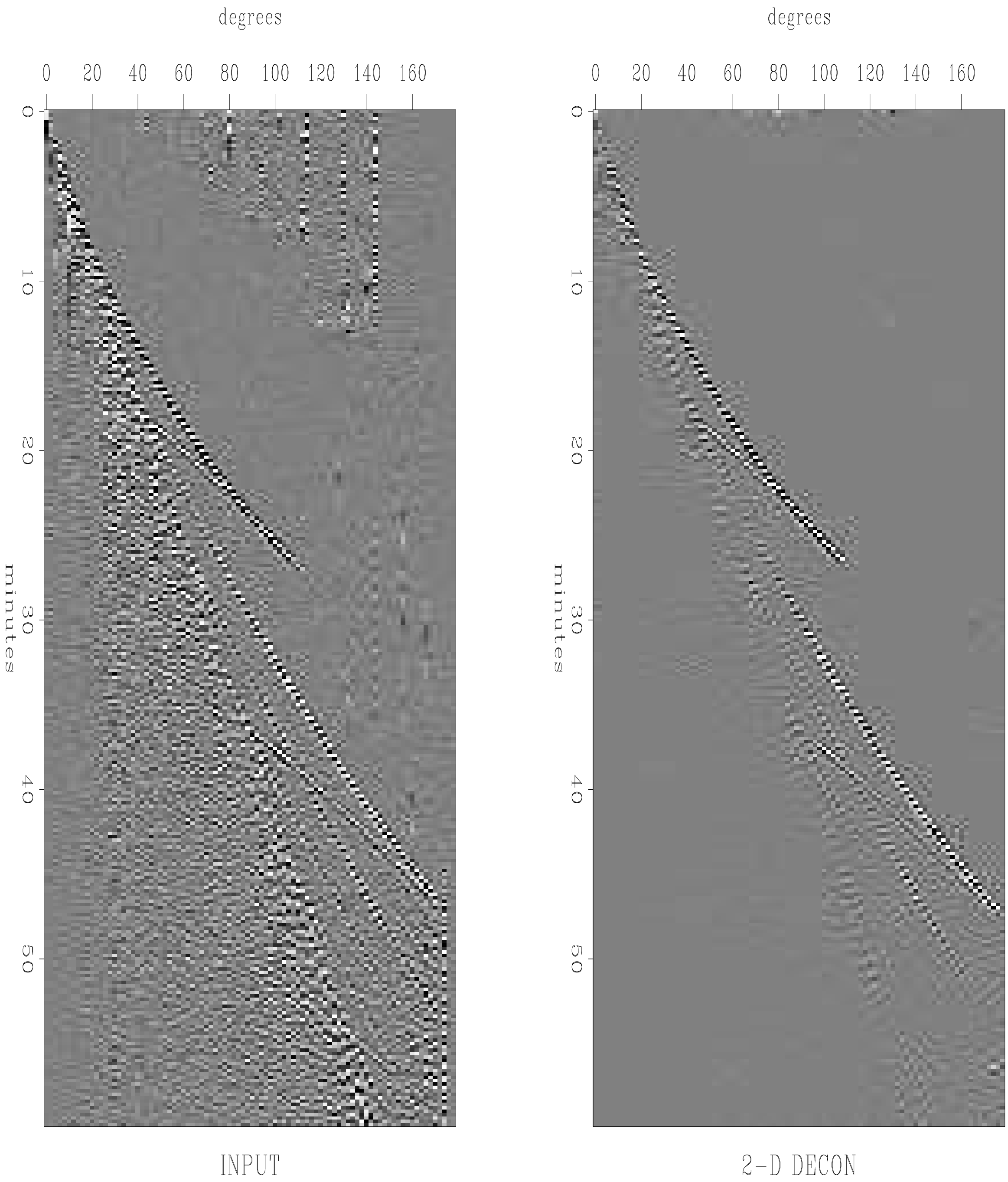

Figure 5: Two-dimensional deconvolution filtering of the horizontal component of the full global image dataset using the a_{11}-constrained filter. Push the button to change the processing parameters and plot a new version of the output. ray2-s2D [ER]

shown in Filter (9).

$$
\begin{array}{ccccc}
a_{1,1} & a_{1,2} & a_{1,3} & a_{1,4} & a_{1,5} \\
\cdot & a_{2,2} & a_{2,3} & a_{2,4} & \cdot \\
\cdot & \cdot & a_{3,3} & \cdot & \cdot \\
\cdot & \cdot & \cdot & \cdot & \cdot \\
\cdot & \cdot & \cdot & \cdot & \cdot \\
\cdot & \cdot & 1 & \cdot & \cdot
\end{array} \tag{9}
$$

Steep-dip deconvolution allows events with velocities slower than the velocities of the desired events to be eliminated. Ground roll and water arrivals may be eliminated with this process.

SPECULATIONS ON THE USE OF VARIOUS FILTER SHAPES

Here we propose a number of other possible filter shapes and their corresponding applications.

Claerbout's LOMOPLAN filter might be replaced with an a_{11} constrained version of the filter as shown in Filter (10) if no prediction is needed along the time axis.

$$
\begin{array}{cc}
\cdot & a_{12} \\
\cdot & a_{22} \\
1 & a_{32} \\
\cdot & a_{42} \\
\cdot & a_{52}
\end{array} \tag{10}
$$

The action of the process is unlikely to change much if a time deconvolution is done first, but the number of coefficients to be calculated would be reduced somewhat.

Where Claerbout's steep-dip deconvolution does both the traditional single trace deconvolution in time plus the removal of steeply dipping events with a single process, I propose a separate removal of the undesired dipping events. A prediction process might use a filter such as shown here

$$
\begin{array}{ccccc}
\cdot & \cdot & \cdot & \cdot & a_{15} \\
\cdot & \cdot & a_{23} & a_{24} & a_{25} \\
1 & a_{32} & a_{33} & a_{34} & a_{35} \\
\cdot & \cdot & a_{43} & a_{44} & a_{45} \\
\cdot & \cdot & \cdot & \cdot & a_{55}
\end{array} \tag{11}
$$

to predict events within a desired range of dips.

Another approach, that of predicting and removing undesired events might be to apply a filter shaped like that of Filter (12).

$$
\begin{array}{ccccc}
a_{11} & a_{12} & a_{13} & a_{14} & a_{15} \\
a_{21} & a_{22} & a_{23} & a_{24} & \cdot \\
a_{31} & a_{32} & a_{33} & \cdot & \cdot \\
a_{41} & a_{42} & \cdot & \cdot & \cdot \\
1 & \cdot & \cdot & \cdot & \cdot \\
\cdot & a_{62} & \cdot & \cdot & \cdot \\
\cdot & a_{72} & a_{73} & \cdot & \cdot \\
\cdot & a_{82} & a_{83} & a_{84} & \cdot \\
\cdot & a_{92} & a_{93} & a_{94} & a_{95}
\end{array}
\tag{12}
$$

This filter shape is likely to produce results similar to the steep-dip deconvolution technique, since the lower four rows of the filter could be understood to eliminate events predicted by the upper-right portion of the steep-dip deconvolution filter.

Another method of modifying the prediction quality is to introduce a gap between the output point of the filter and the free coefficients. For instance, Filter (11) might be modified to appear as

$$
\begin{array}{ccccccc}
\cdot & \cdot & \cdot & \cdot & \cdot & \cdot & a_{15} \\
\cdot & \cdot & \cdot & \cdot & a_{23} & a_{24} & a_{25} \\
1 & \cdot & \cdot & a_{32} & a_{33} & a_{34} & a_{35} \\
\cdot & \cdot & \cdot & \cdot & a_{43} & a_{44} & a_{45} \\
\cdot & \cdot & \cdot & \cdot & \cdot & \cdot & a_{55}
\end{array} .
\tag{13}
$$

This gap would prevent the nearby samples from contributing to the output, forcing the prediction to be done with events that were coherent over a longer distance. While I (Abma) have tried a few tests using small gaps in the filter in the lateral prediction problem, I found only small effects on the prediction.

To remove events with a limited velocity range, filters such as

$$
\begin{array}{ccccc}
\cdot & \cdot & \cdot & \cdot & a_{15} \\
\cdot & \cdot & \cdot & \cdot & \cdot \\
\cdot & \cdot & \cdot & \cdot & \cdot \\
\cdot & \cdot & \cdot & \cdot & \cdot \\
1 & \cdot & \cdot & \cdot & \cdot \\
\cdot & \cdot & \cdot & \cdot & \cdot \\
\cdot & \cdot & \cdot & \cdot & \cdot \\
\cdot & \cdot & \cdot & \cdot & \cdot \\
\cdot & \cdot & \cdot & \cdot & a_{95}
\end{array} ,
\quad
\begin{array}{ccccc}
\cdot & \cdot & \cdot & \cdot & a_{15} \\
\cdot & \cdot & \cdot & \cdot & a_{25} \\
\cdot & \cdot & \cdot & \cdot & \cdot \\
\cdot & \cdot & \cdot & \cdot & \cdot \\
1 & \cdot & \cdot & \cdot & \cdot \\
\cdot & \cdot & \cdot & \cdot & \cdot \\
\cdot & \cdot & \cdot & \cdot & \cdot \\
\cdot & \cdot & \cdot & \cdot & a_{85} \\
\cdot & \cdot & \cdot & \cdot & a_{95}
\end{array} ,
\quad
\begin{array}{ccccc}
\cdot & \cdot & \cdot & \cdot & a_{15} \\
\cdot & \cdot & \cdot & a_{24} & a_{25} \\
\cdot & \cdot & \cdot & \cdot & \cdot \\
\cdot & \cdot & \cdot & \cdot & \cdot \\
1 & \cdot & \cdot & \cdot & \cdot \\
\cdot & \cdot & \cdot & \cdot & \cdot \\
\cdot & \cdot & \cdot & \cdot & \cdot \\
\cdot & \cdot & \cdot & a_{74} & a_{85} \\
\cdot & \cdot & \cdot & \cdot & a_{95}
\end{array} ,
\text{ or }
\begin{array}{ccccc}
\cdot & \cdot & \cdot & \cdot & a_{15} \\
\cdot & \cdot & \cdot & a_{24} & \cdot \\
\cdot & \cdot & a_{33} & \cdot & \cdot \\
\cdot & a_{42} & \cdot & \cdot & \cdot \\
1 & \cdot & \cdot & \cdot & \cdot \\
\cdot & a_{62} & \cdot & \cdot & \cdot \\
\cdot & \cdot & a_{73} & \cdot & \cdot \\
\cdot & \cdot & \cdot & a_{84} & \cdot \\
\cdot & \cdot & \cdot & \cdot & a_{95}
\end{array}
$$

might be used. The form of the filter would depend on the known velocity range of the undesired events and how well the position of the coefficients fit the events. If the $a15$ and $a95$ coefficients fit the velocity of the undesired events perfectly, only these two coefficients would be needed. In general, since the grid on which the coefficients sit would not fit a given velocity, the second filter with $a15$, $a25$, $a85$, and $a95$ free would be needed. If more than one event within the velocity range exists, or if events dipping both directions with the same velocity exist within a window, more columns with free coefficients will be needed. The last of the previous filters may be needed in a practical case.

For the lateral prediction problem, the optimum filter shape is unclear. Ideally, a small filter with few coefficients is desired. As discussed above, a tall narrow filter such as Filter (8) would predict a single linear event. Adding more columns, such as in Filter (1) would allow more linear vents to be predicted. The number of time coefficients might be determined by the maximum dip expected. The safest filter, one with a large number of columns and rows, might be too expensive to calculate practically.

One might assume that a filter which is symmetric about the time and space axes would not require two passes of prediction. However, this is not the case. First, the calculation of Filter (14) shown below should be symmetric about the central coefficient, so calculating the other coefficients might be considered a waste of time.

$$\begin{array}{ccccccccc} a_{11} & \cdot & \cdot & \cdot & \cdot & \cdot & \cdot & \cdot & a_{19} \\ a_{21} & a_{22} & a_{23} & \cdot & \cdot & \cdot & a_{27} & a_{28} & a_{29} \\ a_{31} & a_{32} & a_{33} & a_{34} & 1 & a_{36} & a_{37} & a_{38} & a_{39} \\ a_{41} & a_{42} & a_{43} & \cdot & \cdot & \cdot & a_{47} & a_{48} & a_{49} \\ a_{51} & \cdot & \cdot & \cdot & \cdot & \cdot & \cdot & \cdot & a_{59} \end{array} \tag{14}$$

A second, more important issue is that Filter (14) looks like an interpolation-error filter. In Claerbout's(1992) discussion of one-dimensional interpolation-error filters, the output is shown to have spectrum that is the inverse of the input. This is generally undesirable. Therefore, the filters we generate will be one-sided in either time or in space.

As seen in the examples above in Filters (6) and (7), a filter with no free coefficients in the output column appears to have a forward prediction filter that is simply the reverse of the reverse prediction. This is not true with the filter with free coefficients in the output column.

While calculating small filters might be efficient, calculating larger filters involves n^3 operations, where n is the number of coefficients to be calculated. Breaking large filters into smaller ones might reduce the computation significantly.

CONCLUSIONS

We have shown how two-dimensional lateral-prediction filtering can provide an improvement over the results of FX-decon and we have shown how FX-decon is equivalent to a two-dimensional filter with a long length in time. We have shown some of the effects of the different configurations of two-dimensional filters and how we built different applications based on the filter actions. We are just starting to understand the possible applications of multi-dimensional filters. They appear to have a flexibility that other techniques do not. The possibility of choosing a filter shape to control the action of the filter may allow many new applications within the seismic industry. Three applications mentioned here have been implemented; many more are likely.

REFERENCES

Abma, R., 1993, Lateral prediction techniques: FX-decon versus Two-D deconvolution: SEP–**77**, 257–270.

Canales, L. L., 1984, Random noise reduction: 54th Annual Internat. Mtg., Soc. Expl. Geophys., Expanded Abstracts, Session:S10.1.

Claerbout, J. F., 1992a, Earth Soundings Analysis: Processing Versus Inversion: Blackwell Scientific Publications.

Claerbout, J. F., 1992b, Information from smiles: Mono-plane-annihilator weighted regression: SEP–**73**, 409–420.

Claerbout, J. F., 1993, Steep-dip deconvolution: SEP–**77**, 245–256.

Gulunay, N., 1986, Fx decon and complex wiener prediction filter: 56th Annual Internat. Mtg., Soc. Expl. Geophys., Expanded Abstracts, Session:POS2.10.

Shearer, P., 1991, Imaging global body wave phases by stacking long-period seismograms: Journal of Geophysical Research, **96**, 535–555.